

Regional hydrologic and ecologic characterization and  
baseline assessment of remote northern Canadian terrain in  
advance of shale oil and gas development

Third Annual Report to:

NWT ESRF Management Board



By:

**David Rudolph**

University of Waterloo

June, 2020

## 1.0 INTRODUCTION

The Year 3 work activities associated with the project have been focused on: **1).** Ground truthing field measurements to support and verify the identification of groundwater phenomena based on the satellite optical imagery and low-elevation thermal imagery completed at the Husky Slater River lease areas; **2).** coordinate and expedite a focused regional summer water sampling and field monitoring campaign with Husky personnel; **3).** combine inorganic and organic geochemical data with environmental isotope data to characterize surface and groundwater flow phenomena within the deep and shallow groundwater flow systems at the site and **4).** Develop a new mathematical modeling tool to study groundwater flow in discontinuous permafrost environments.

Following the approach established during Years 1 and 2 of the project, the majority of the field activities undertaken in Year 3 were focused within the Bogg Creek Watershed shown in Figure 1.

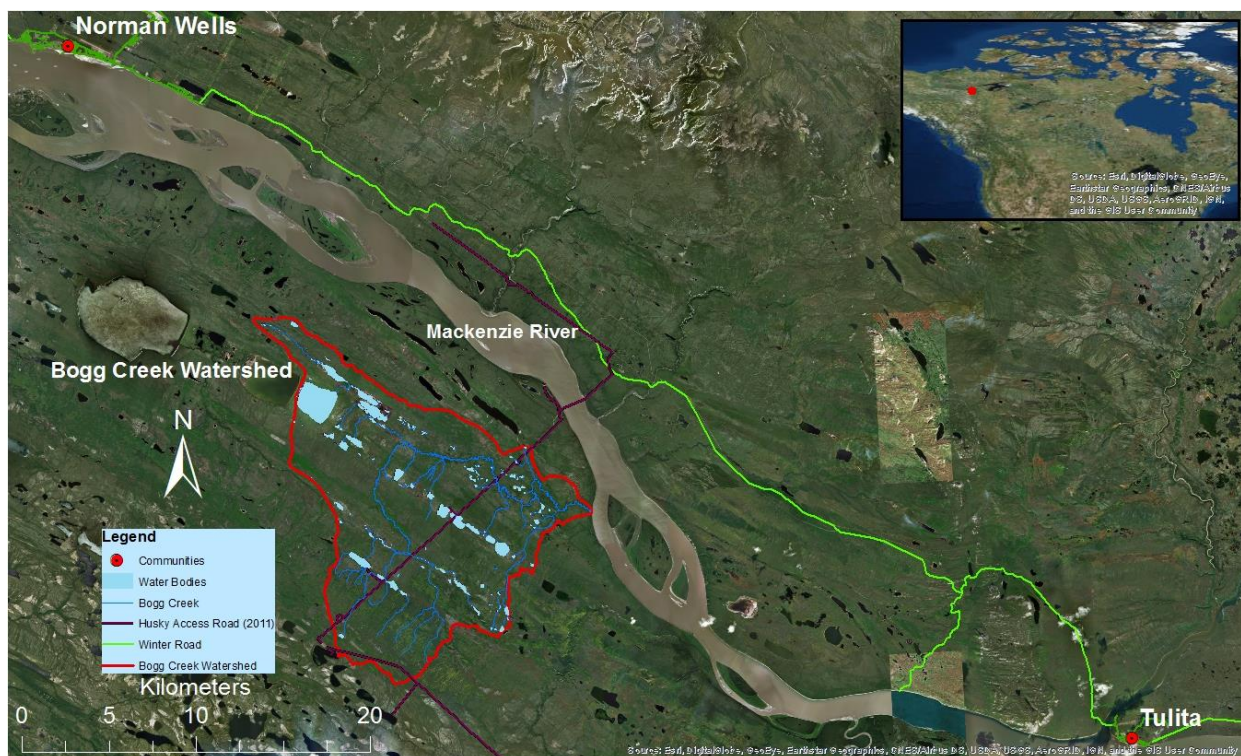


**Figure 1:** Satellite photo of Bogg Creek study area and surrounding communities of Norman Wells and Tulita. Inset map showing Canada and position of study area.

As defined in previous reports, the Bogg Creek subwatershed is situated within Husky’s Slater River Lease region, which is part of the Sahtu Settlement Area (SSA). Since 2013, Husky environmental teams have conducted regional baseline monitoring in and around the Bogg Creek watershed, and this historical data have proven invaluable in understanding the hydrologic characteristics of this area within the Central MacKenzie Valley. As part of this current project, we continue to build on this data set and collaborate with Husky in expanding the knowledge base in this region.

In Year 3, the field activities associated with this project benefitted from technical, financial and in kind support from research colleagues from Wilfred Laurier University (WLU) and Husky personnel. The financial and in kind support were primarily leveraged through our on-going research work supported

through the Global Water Futures (GWF) program centered at the University of Saskatchewan. The specific research programs involved include the Northern Water Futures study headed by Dr. Jenn Baltzer at WLU and the Transformative Sensors and Smart Watersheds (TSSW) project headed by Drs. Claude Duguay and Dave Rudolph and the University of Waterloo. Husky Energy provided some helicopter support, facilitated access to their lease sites, provided field supervision and safety support and have shared all of their field data with our team.

Based on initial discussions with Husky, the intention is for the all-season access road to remain available for use during the 2020 field season and potentially longer into the future. However, the limitations associated with the Covid-19 pandemic will likely result in the need to postpone the planned field activities for the 2020 season until access to the NWT is permitted by health authorities

As in previous annual reports, progress on each of the Year 3 topic areas listed above will be summarized in separate sections below.

## 2.0 Ground Truthing of Remotely Identified Groundwater Flow Phenomena

The remote sensing methods and interpretation procedures used within the Bogg Creek Watershed to locate icings using optical and thermal satellite imagery is explained in detail in the MSc thesis of Glass (2019) and associated journal article by Glass et al., 2020, following the methods developed by Morse and Wolfe (2015). The identification of icings was performed with the use of Landsat 4-5 Thematic Mapper (TM) and Landsat-8 Operational Land Imager (OLI) optical imagery, RapidEye-3 optical imagery, and Landsat 4-5/8 120 m thermal imagery for various years with available data that would be appropriate for assessment. Utilizing the algorithm processes developed by Morse and Wolfe (2015), late spring imagery from each of these years was used to identify areal icing coverage. The icing coverage from multiple years can be compared to locate areas where they consistently occur, which is indicative of a perennial spring area. The icing maps generated in this fashion within the Bogg Creek Watershed is shown in Figure 2 (Glass, 2019; Glass et al., 2020, Wicke and Rudolph, 2020).

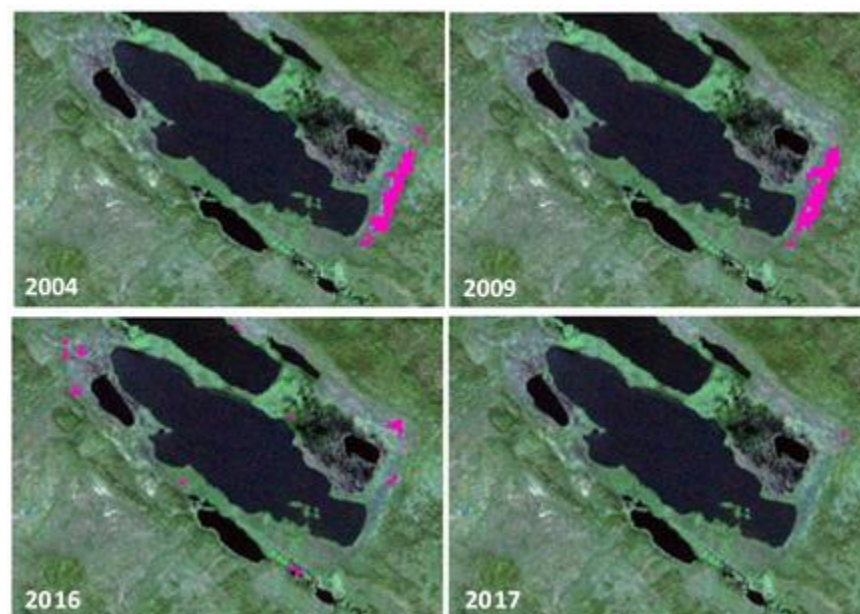


**Figure 2:** Location of an icing cluster within the Bogg Creek Watershed between 2004-2017 (icings shown in pink) (from Glass, 2019 and Glass et al., 2020) modified from Rudolph (2019).

In addition, groundwater emerging through seeps and springs with enough temperature difference from the surrounding surface water or nearby vegetation can be detected with IR cameras (Rudolph, 2019; Wicke and Rudolph, 2020). This technology is most useful when paired with a helicopter flying at low elevation, allowing rapid characterization of groundwater discharge locations over a large area. The data collected during Year 2 of the project were processed and analyzed to inform the selection of specific field monitoring sites. Some specific examples of cold anomalies and potential springs from the Bogg Creek watershed are illustrated in Figure 2.

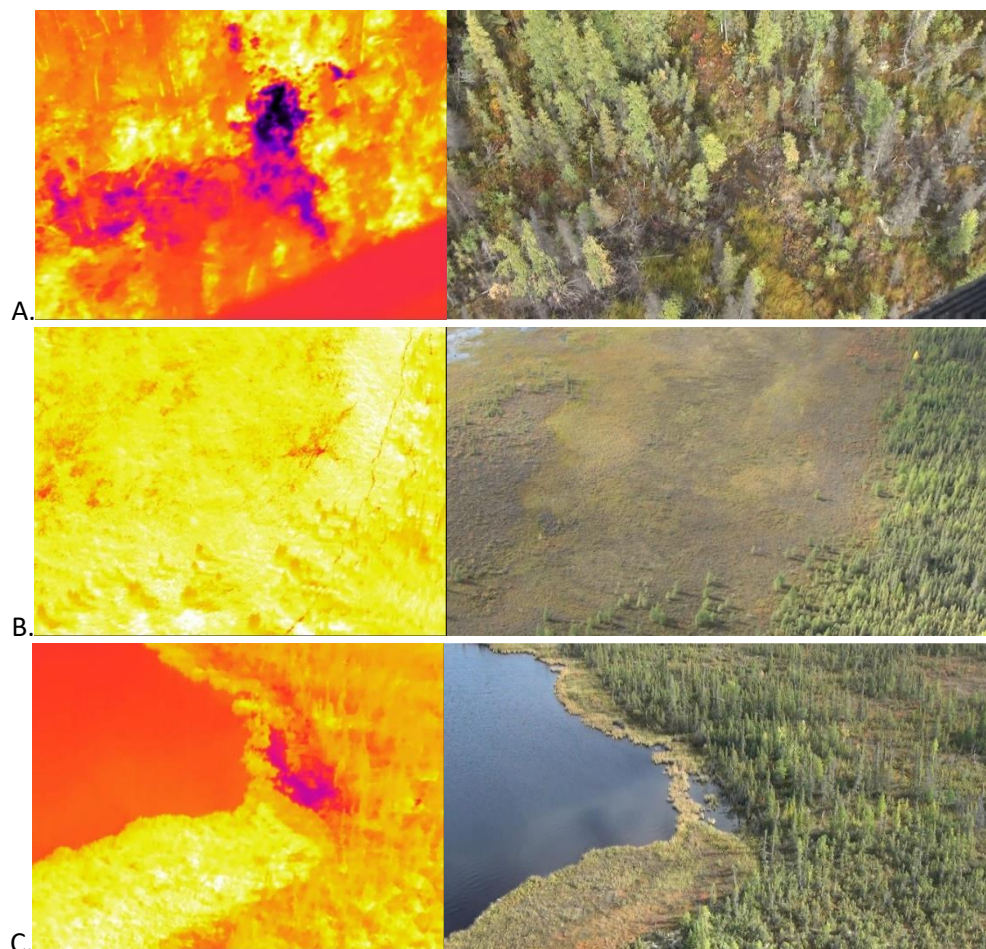


**Figure 3:** A): A large cold anomaly within a seismic cutline. B): Two thermal anomalies in a wetland adjacent to a lake. C): Thermal anomaly from spring-fed water pooling on the sides of a lake. Photos by B. Conant Jr.

During the second year of the project, we were able to confirm the utility of optical satellite imagery (Landsat 4-5 TM and RapidEye-3) and low-altitude aerial thermal infrared (TIR) to detect groundwater discharge locations through icing identification through ground truth data collection. This included measurements of vertical hydraulic gradients, geochemical and isotopic data and terrestrial geophysical surveying of the locations identified by the remote sensing collected during field work at the Bogg Creek observatory. This approach will help to identify locations of groundwater discharge and changes in these conditions based on remote sensing tools.

Data collected at these specific field sites are described in more detail below.

## **2.0 Regional Summer Water Sampling and Field Monitoring and Laboratory Work**

### **2.1 Water Sampling**

The Year 3 fieldwork took place late in August, 2019. This campaign aimed at obtaining permafrost cores, expanding the number of surface water monitoring locations along Bogg Creek and its tributaries and revisiting spring locations (Figures 1, 2 and 3). Travelling with Husky personnel, 27 surface water locations were visited, with stable water isotope samples being obtained from 14 of them. Samples for  $^{87}\text{Sr}/^{86}\text{Sr}$  were obtained from locations within the Bogg Creek watershed during this time as well. A total of 11 new sampling locations were selected based on presence of thermal anomalies and to provide additional coverage of the creek and its tributaries. Springs around the lake region shown in Figure 2 and identified with remote sensing data were revisited to obtain duplicate samples and to attempt to take a geochemical profile from several depths. Husky Oil Operations directly provided data to the University of Waterloo, including 2016-2019 water geochemical data and thermistor readings spanning the time of installation (2013) to when they were removed (2019). Some of the major findings of this data are shown in subsequent sections.

### **2.2 Permafrost Coring and Porewater Extraction**

Permafrost coring was performed using a modified Stihl gas powered auger borrowed from the Northwest Territories Geological Survey. Approximately 2 m long cores were taken from two locations along the all-weather access road (MW04 and H040), with a duplicate core taken from H040. At the time of the current reporting, data from the H040 core was available to report. Cores were taken in 10-20 cm intervals, logged for sediment and permafrost characteristics, bagged with zip-top plastic bags and placed in a cooler with ice packs. The core was then kept frozen and transported to the University of Waterloo. Each section was resealed into new plastic zip-top bags which were wrapped tightly around the core to minimize the amount of air available to cause unwanted fractionation of liquid or frozen water. As much excess air was removed as possible by squeezing the bag, which was then placed inside another closed plastic bag. These were then left to sit out at room temperature for 18-24 hours or until completely thawed.

Porewaters were extracted using methods outlined in Moncur et al., (2013). This method utilizes a hydraulic jack and custom-built squeezing tubes to contain the core and allow for sampling with a syringe. Compressional pressure is generated by the jack and by suction from the syringe. Squeezed water was filtered twice through  $0.45\ \mu\text{m}$  syringe filters to remove any organics or fine material, once during squeezing and again after sample collection. Similar protocols for field water sampling were used in the collection of these porewaters. Cores were analyzed for major and minor ions as well as stable water isotopes.

## **3.0 Geochemical, Isotopic and Ground Temperature Analysis**

Through a combination of inorganic and organic geochemical analysis and environmental isotope data from surface and groundwater within the field study site, deep and shallow groundwater flow systems could be detected and characterized within a discontinuous permafrost terrain. These types of data are extremely rare in this type of remote northern terrain and specifically as they were used to understand regional hydrogeology. These data and analytical techniques can be applied throughout the northern Canadian landscape to evaluate groundwater flow systems and to establish baseline hydrologic conditions

prior to resource development of the construction of infrastructure. The major results associated with the geochemical and isotopic analyses are provided below.

A piper plot with all creek and water source endmember data is shown below in Figure 4. Lower reaches of Bogg Creek retain a similar geochemical pattern that varies seasonally, while two tributaries show the influence of greatly different water sources with similar seasonal variability. Generally, lower reaches appear to be a mixture between Na-Cl, Na-HCO<sub>3</sub> waters (subpermafrost groundwater) and with some inputs of Ca-SO<sub>4</sub> and Ca-HCO<sub>3</sub> waters (possibly runoff and suprapermafrost waters).

Samples collected during more rainy periods or early in the year generally show higher influences of runoff and suprapermafrost waters, reflecting increased inputs of shallower water and surface runoff. Samples during drier periods and later in the summer generally reflect less influence from shallow inputs and show a stronger subpermafrost component. Differences between two of the sampled tributaries can be observed, one plotting between the suprapermafrost and runoff endmembers, dominated by Ca-HCO<sub>3</sub>, and another overlapping on the Na-HCO<sub>3</sub> subpermafrost endmember. This indicates that one tributary is driven primarily by shallow groundwater flow and runoff, while the other is fed mostly by subpermafrost groundwater. Seasonal and yearly variation is also apparent in these samples, following similar patterns as the lower reaches.

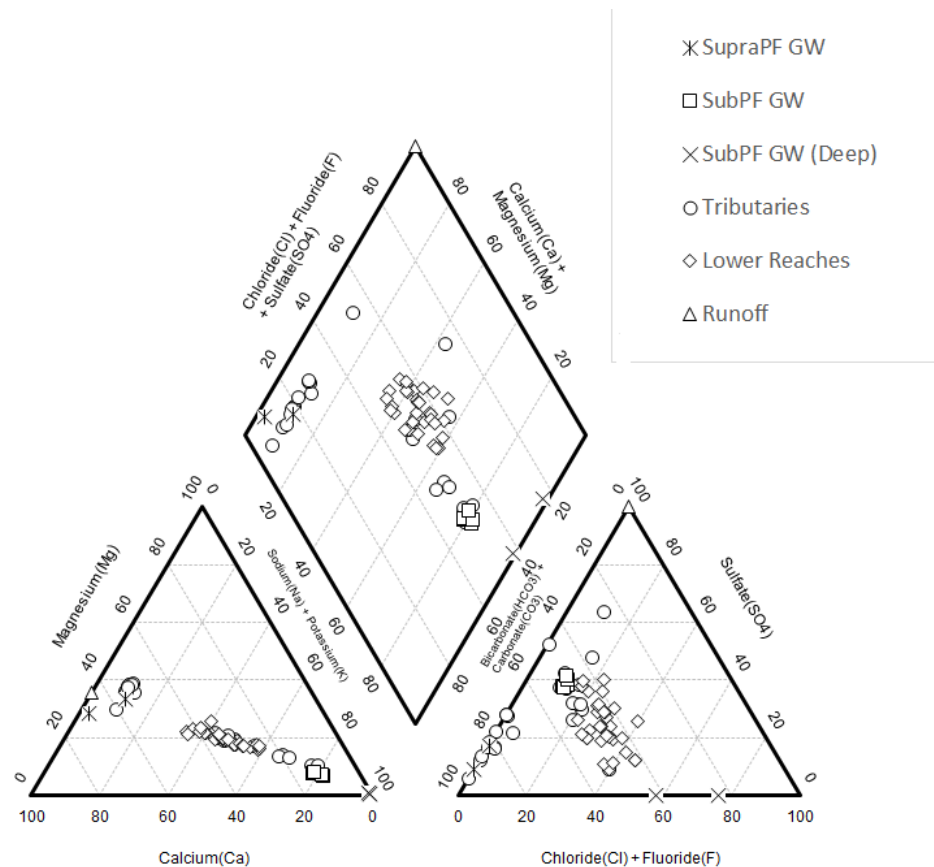


**Figure 4:** Piper plot of site wide groundwater and stream water. Tributaries show distinct overlap with certain endmembers and some variability due to different contributions of runoff and groundwater. Lower reaches appear to be mixtures of several endmembers and so do not overlap but vary due to different proportions of runoff and groundwater. Some data provided directly from Husky Energy or obtained from Husky Oil Operations Ltd (2016) and Waterline Resources Inc., (2013a, 2013b).

The groundwater spring geochemistry is shown below in Figure 5. Two main springs were identified around the lake complex shown in Figure 2 as described earlier, and were labeled GL and GPH for reference. Three sites at GL were sampled, GL1 and GL2 in 2018 and GL3 in 2019. In 2018 the GL samples were quite similar, plotting mostly as Ca/Na-HCO<sub>3</sub> type waters with high Cl and low SO<sub>4</sub>. In 2019 GL3 was similar but had more Ca and HCO<sub>3</sub> than the previous sites in 2018. This water appears to be the result of mixing of two water sources such as subpermafrost and suprapermafrost waters or has had a complex geochemical evolution. It is known that saltier overburden has been found in the field site (Waterline Resources Ltd., 2013a) and is not unique to just subpermafrost groundwater. The second spring location, GPH was sampled in 2 locations, GPH1 in 2018 and GPH2 in 2019. Geochemistry was vastly different for these two locations, with GPH1 characterized by mostly Ca-SO<sub>4</sub>, likely reflecting water interaction with pyrite in shales (slightly deeper flow path) and/or flow through sulphur rich peat (shallow flow path). GPH2 was dominated by Ca-HCO<sub>3</sub>, reflecting a suprapermafrost flow path.

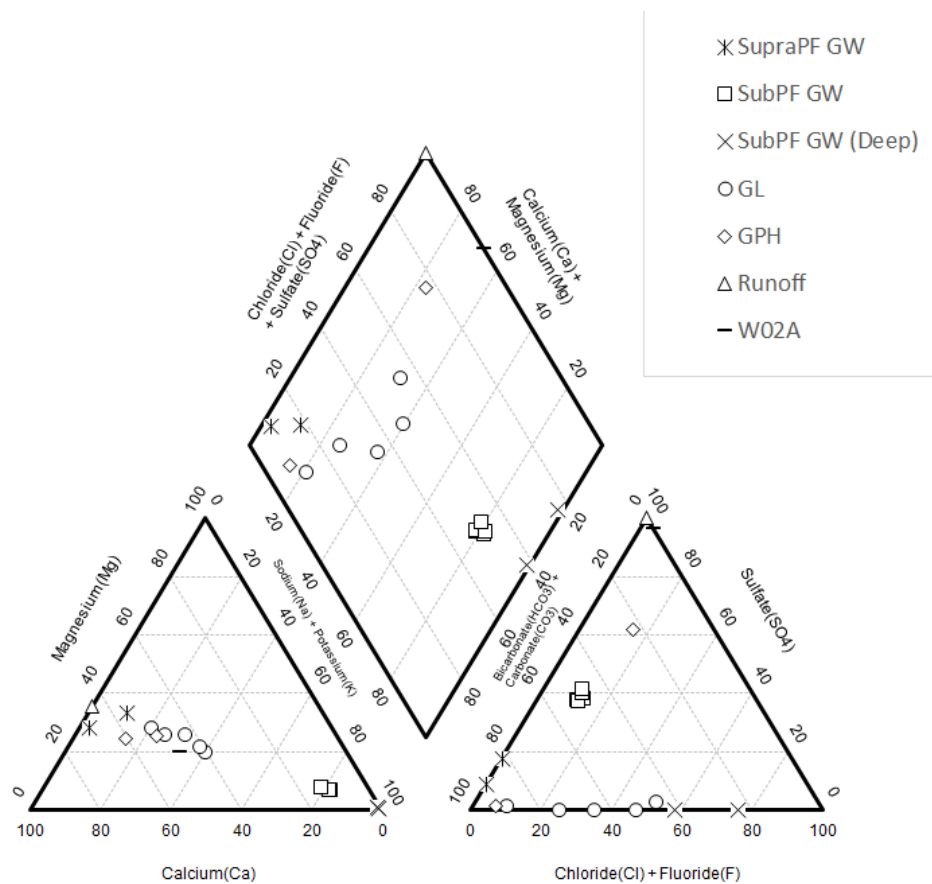


**Figure 5:** Spring geochemistry plotted on a piper diagram. Spring geochemistry reflects complex flow paths with several explanations for their origin. Endmember data from and Waterline Resources Inc., (2013a, 2013b)

Results from  $\delta^{18}\text{O}$  and  $\delta^2\text{H}$  of all waters in the watershed for all years are shown below in Figure 6. The most important aspects are that surface water generally experiences some evaporative enrichment, plotting on the Local Evaporation Line (LEL), however some surface waters plot along the Local Meteoric Water Line (LMWL), indicating a balance between new inputs and evaporation. Groundwater and spring  $\delta^{18}\text{O}$  and  $\delta^2\text{H}$  values are variable but typically plot along the LMWL. Groundwater and springs have an

average that reflects the weighted annual average of precipitation. Some that are more associated with surface water or are mostly fed by rainwater plot above this average, while others plot below this average, reflecting a recharge source that is lighter isotopically. This could indicate a component of ancient groundwater (as was observed for the lightest samples), snow or permafrost melt water in these lighter waters.

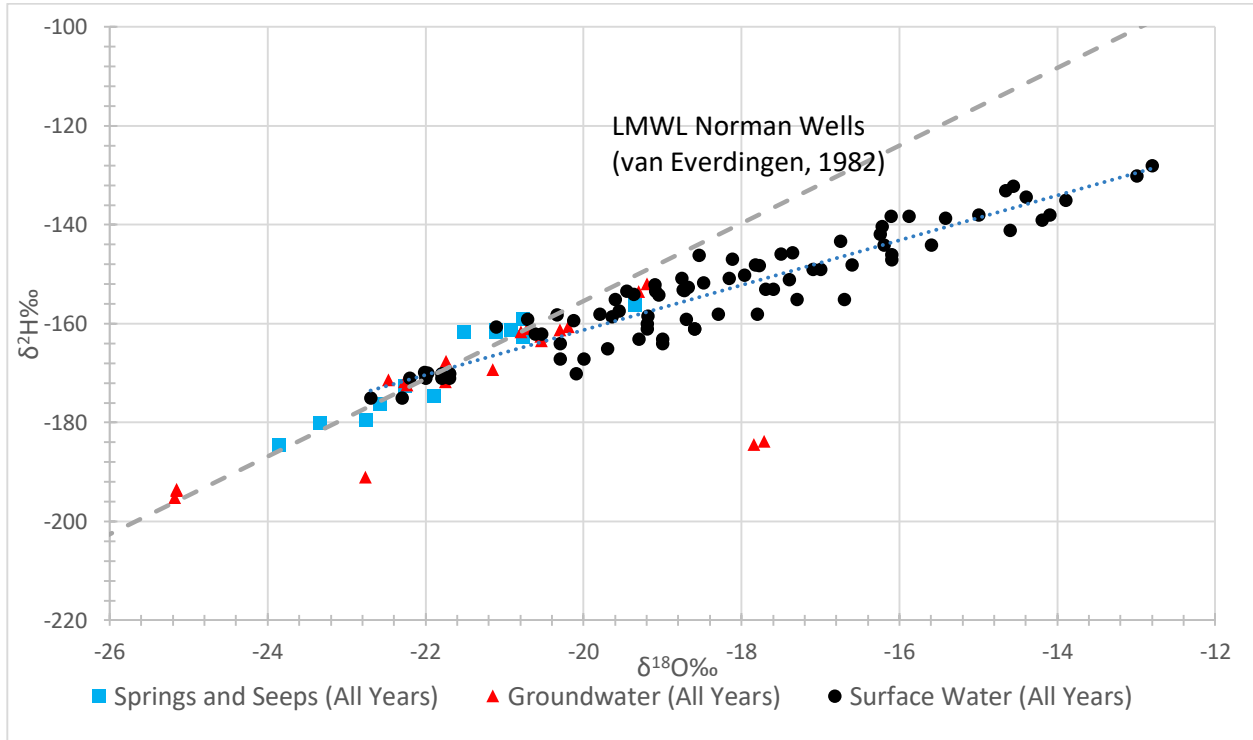


**Figure 6:**  $\delta^{18}\text{O}$  and  $\delta^2\text{H}$  data from 2012, 2018, and 2019 from around Bogg Creek and its surrounding area. Typically, groundwater (red) plot closer to the weighted average for precipitation, but some fall above or below. This case is also true for seeps and springs (blue). Surface water (black) generally shows an evaporated signal and falls on the LEL. Some data retrieved from AMEC, (2013) and Husky Oil Operations Ltd., (2016).

Strontium concentrations and isotopes ( $^{87}\text{Sr}/^{86}\text{Sr}$ ) are shown below in Figure 7. Spring data are shown as red diamonds and plot close to supraperafrost groundwater endmembers, but fall along a short line. This could indicate mixing of supraperafrost and an unknown endmember or geochemical evolution of supraperafrost groundwater as it takes a deeper flow path. Creek samples generally plot between three endmembers, runoff, winter baseflow and subpermafrost groundwater. In 2019, a relatively dry year, they plot closer to the subpermafrost endmember. Tributary 1 and 2 are also shown as orange circles. Tributary 1 was identified earlier through geochemistry to consist of mostly supraperafrost and

runoff water, which is mostly reflected in the plot. Tributary 2 was identified as consisting mostly of subpermafrost groundwater, which is reflected in the plot as well.

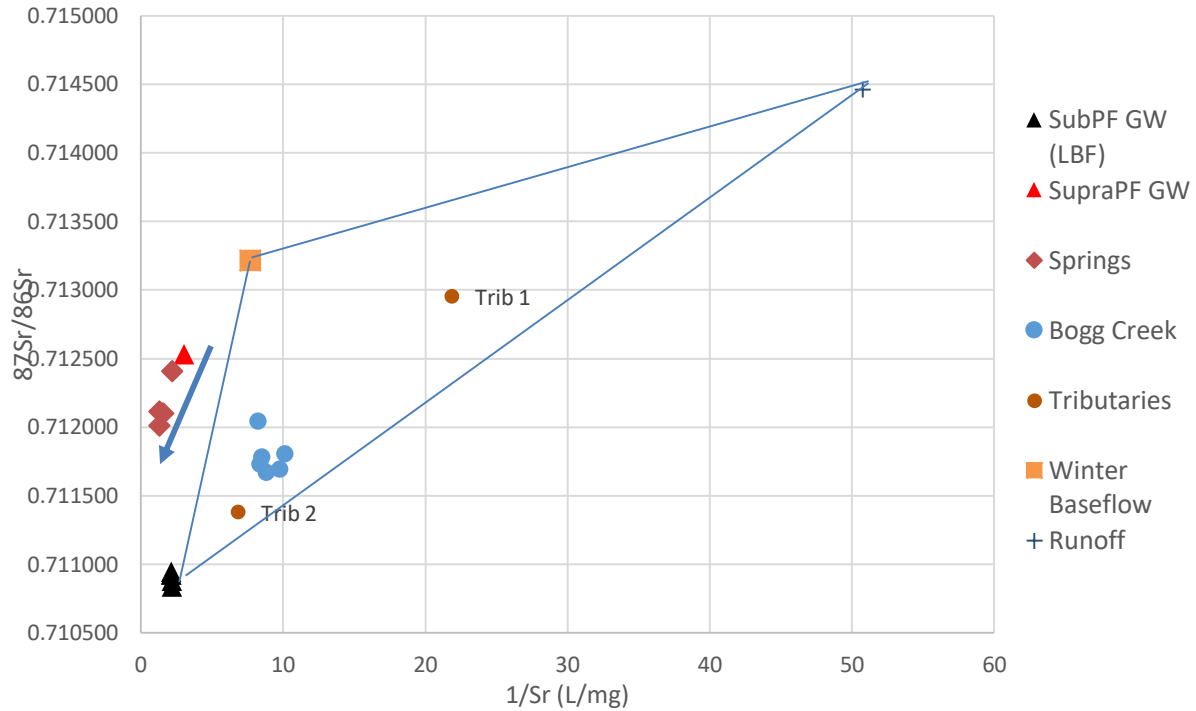


**Figure 7:**  $^{87}\text{Sr}/^{86}\text{Sr}$  vs  $1/\text{Sr}$  for some spring (all years) and creek samples (2019) collected within the Bogg Creek watershed and various endmembers (Wicke, 2020).

Core taken for soil water analysis (referred to as the HO40 site and associated with one of the cleared drilling pads on the Husky lease site) within the permafrost was primarily silt with clay with abundant organics. A small interval of unfrozen active layer bounded on top and bottom by unfrozen soil was observed in the first 30 cm. The actual permafrost table was at a depth of about 50 cm. Porewater geochemistry is shown in Figures 8 and 9 below. Water types ranged from  $\text{Ca-SO}_4$  rich in the active layer to  $\text{Ca-HCO}_3$  rich in the permafrost. What was noticed from these cores was that porewater at the ice-water interface was highly elevated in most solutes, likely reflecting freeze-out of ions during winter, which then concentrate above the permafrost. Secondly, below this interval into the frozen soil, most solutes begin a steady increase in concentration, likely as a result of reduced solute flushing and weathering of these deeper sections of the subsurface. It is hypothesized that future thawing of this ice will begin to release these solutes as groundwater flow is re-activated.

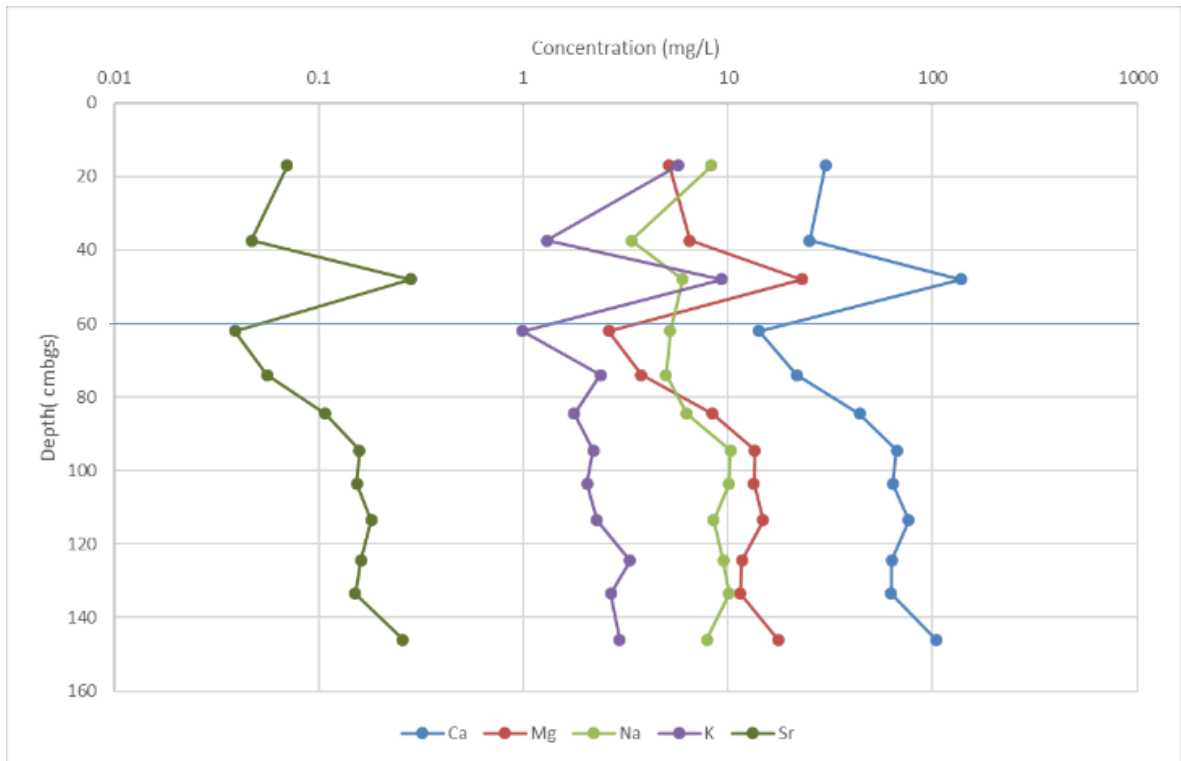


**Figure 8:** Cation concentration (log scale) vs depth in H040 core. Permafrost table is shown as a blue line.

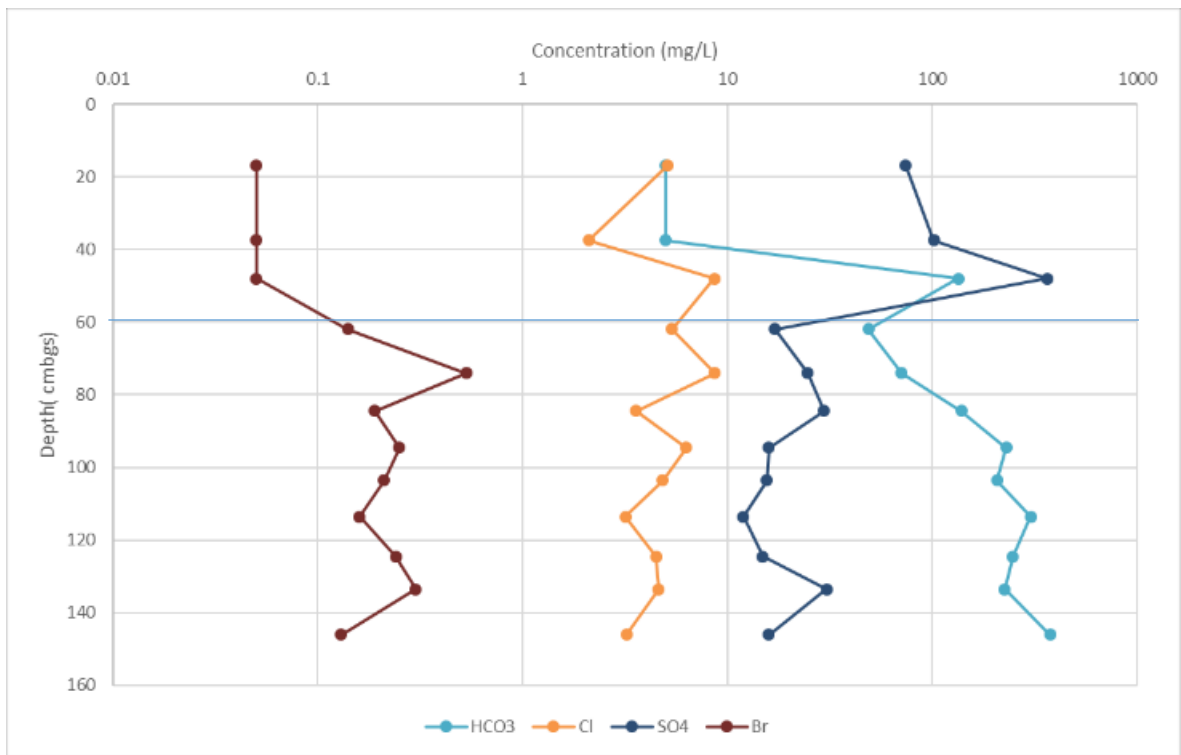


**Figure 9:** Anion concentrations (log scale) vs depth in H040 core. Permafrost table is shown as a blue line.

Stable water isotopes are shown in Figure 10 below. What is revealed is that the first 0-60 cm of core contains modern meteoric water, and below that the water is generally isotopically lighter. Potential influx of evaporated surface water (sample was taken near a lake) at a depth of 125 cm can also be observed, possibly reflecting the freezing history of the permafrost. Permafrost isotopic composition is likely indicative of a colder climate during the formation of this permafrost as these values are much lighter than modern water. It is hypothesized that this may be a contributor to some of the isotopically light groundwater and spring samples.

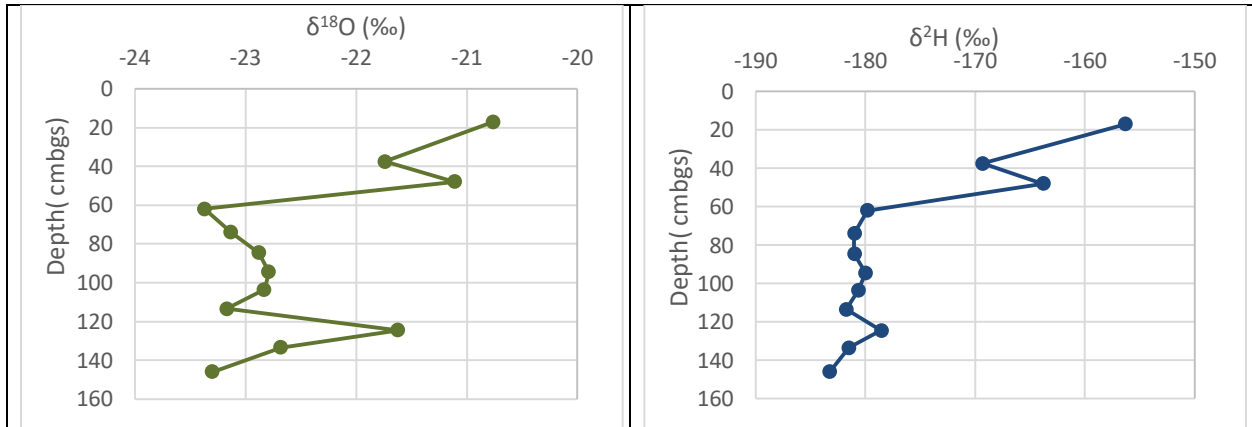


**Figure 10:**  $\delta^{18}\text{O}$  (left) and  $\delta^2\text{H}$  (right) vs depth profiles for H040 permafrost core.

Thermistor data provided directly from Husky Oil operations was used to construct temperature profiles for each year since installation for two thermistor strings, MW01T and MW09T, situated along the all-season road. The combined data are shown in Figure 11. Temperature profiles show the minimum temperatures from all years, and the maximum temperatures for each year starting in early March 2013 (when measurements began) and use the yearly maximum and minimum temperatures to estimate the total depth of thaw. Profile MW01T shows a relatively small temperature envelope between minimum and maximum temperatures. Most of the variance in the temperature differences occurs in the top intervals, narrowing with depth due to dampened temperature effects. A small increase in temperature at depths 2.75-10.75 m can be observed each year, although temperatures do not exceed  $0^\circ\text{C}$ . In fact, thaw depth in this profile seems to not change until 2017-2018 where thaw depth decreases slightly. Minimum temperatures did not change from year to year, peaking in 2013.

Comparatively, MW09T shows a dramatic increase in thaw depth every year, changing from 1.5 m to  $>4.5$  m between 2013 to 2018. MW09T was not installed quite as deep as MW01T and so the point at which the ground temperature remains stable is not visible. This thermistor appears to record a very dramatic warming of ground temperatures and a thawing of permafrost. The most dramatic change in thaw depth was between 2015-2017, with a 1.5 m increase in active layer thickness. Like MW01T minimum temperatures peaked in 2013 and then did not decrease in subsequent years.

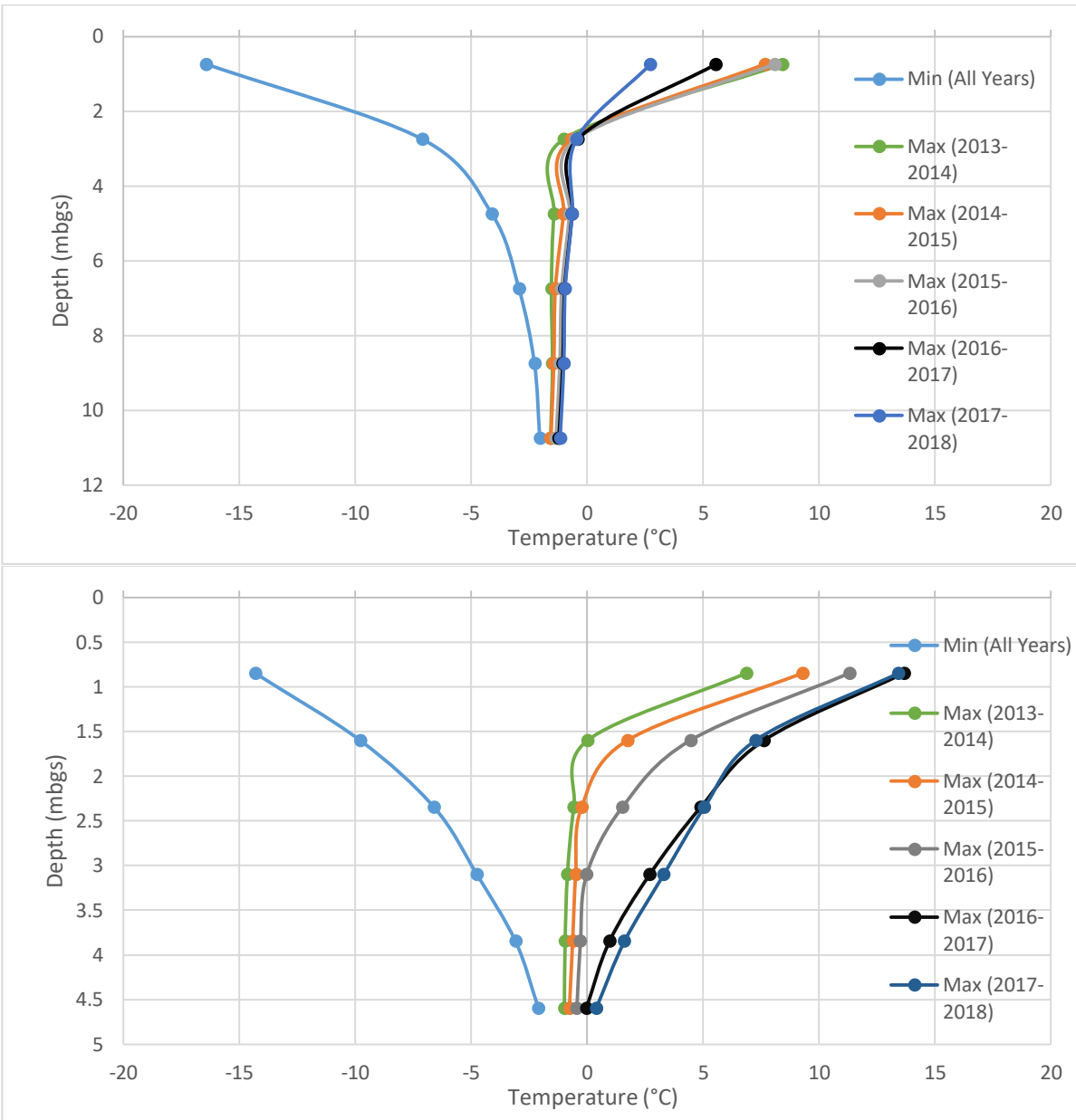


**Figure 31:** Temperature vs Depth profiles for MW01T (top) and MW09T (bottom). Both profiles show a warming trend in their lower intervals but only MW09T shows a change in the thaw depth (active layer) base.

These differences in thaw depth changes between each thermistor are unexpected, as MW09T seems to represent an extreme example of increased summer energy flux into the ground and decreased winter energy flux out of the ground, thawing the ground considerably. Contrastingly, MW01T shows much more modest warming below the permafrost table and cooling above this point. Installation of these thermistors involved clearing of land of vegetation to form a pad, with a layer of mulched vegetation laid down over top of soil to act as insulation. This insulation appears to be working well in MW01T but not in MW09T. This may be due to the thermal properties of the different overburden materials. MW01T was installed into primarily silt and silty sand, while MW09T is installed in clayey silt till and shale bedrock. This indicates that thawing is not universal across the watershed but is quite

heterogeneous. In some areas thicker active layers may be generated, increasing the potential volume of aquifer for groundwater flow to occur.

#### **4.0 Mathematical Modeling**

During the Year 3 program year, new numerical solutions to the problem of fully coupled thermal-hydraulic-mechanical (THM) processes as related to soil freeze and thaw dynamics have been developed and verified through comparison with literature experimental data. The model development has specifically focused on the problem of freezing and thawing soils in partially saturated conditions. The new modeling platform has been completed and applied to the problem of the influence of soil freezing on buried infrastructure including pipelines as an initial test case (Huang et al. 2020). This has applications for threats to buried petroleum pipeline infrastructure in the north.

The newly developed THM algorithms are being coupled with 3D variably saturated groundwater flow and transport models (FeFlow and HydroGeoSphere) with the objective of utilizing them to investigate seasonal freeze-thaw dynamics and active zone processes related to short and medium-term permafrost degradation. This modeling approach is intended to facilitate the consideration of partially saturated flow and transport processes for more complete physical representation of soil water and contaminant movement in the shallow subsurface during freeze-thaw cycles, with a specific application within permafrost terrain. The model is now in early stages of being developed for a simulation of the field conditions within the Bogg Creek watershed, with specific focus on groundwater processes and permafrost degradation as the climate warms.

#### **5.0 Proposed Year 4 Activities**

The planned activities for Year 4 of the project will in part depend on travel restrictions related to the Covid-19 pandemic. We are planning to conduct low-elevation, air borne EM geophysical surveys designed to regionally map the upper and lower boundaries of the permafrost within the Bogg Creek region. We have connected with two geophysical contractors and by combining financial resources from several sources, the air borne geophysical surveys are now feasible. Access to the Norman Wells airport and local facilities, including helicopter services will be necessary and will depend on permission to visit this region by health officials. Should access to the region and field sites be secured, we anticipate a final, very focused field sampling campaign in collaboration with Husky personnel.

In addition to the geophysical surveys, we plan to continue detailed assessment of all of the collected field data, and continue to advance the permafrost monitoring tools and applications for simulation experiments within the Central MacKenzie Valley region.

#### **6.0 References**

AMEC Environment & Infrastructure (2013). Central Mackenzie Valley Subsurface Groundwater Baseline Study. Submitted to the Northwest Territories Geoscience Office, Government of the Northwest Territories.

Glass, B. (2019). Examining Hydrogeological Processes in Freezing Soils using Remote Geophysical and Numerical Techniques [Thesis]. University of Waterloo

Glass, B., Rudolph, D., Duguay, C., and Wicke, A. (2020). Identifying Groundwater Discharge Zones in the Central Mackenzie Valley Using Remotely Sensed Optical and Thermal Imagery. *Canadian Journal of Earth Sciences*. In press, cjes-2019-0169.

Huang, X., Rudolph, D.L., and Glass, B. (2019). Potential influence of roadbed frost load on water main failure, submitted to *Geophysical Research Letters* (in final revision)

Husky Oil Operations Ltd. (2016). 2016 Surface Water Quality Assessment. Tulita District, NT.

Moncur, M. C., Blowes, D. W., & Ptacek, C. J. (2013). Pore-water extraction from the unsaturated and saturated zones. *Canadian Journal of Earth Sciences*, 1058(July), 1051–1058.

Morse, P. D., & Wolfe, S. A. (2015). Geological and meteorological controls on icing (aufeis) dynamics (1985 to 2014) in subarctic Canada. *Journal of Geophysical Research F: Earth Surface*, 120(9), 1670–1686. <https://doi.org/10.1002/2015JF003534>

Rudolph, D. (2019). Regional hydrologic and ecologic characterization and baseline assessment of remote northern Canadian terrain in advance of shale oil and gas development Second Annual Report to: NWT ESRF Management Board. Waterloo ON.

Wicke, A. (2020). Characterizing Aspects of Groundwater Flow in a Discontinuous Permafrost Region, Sattu Settlement Area, NT [Thesis]. University of Waterloo, in progress.

Wicke, A. and Rudolph, D. L., (2020). Hydrogeological Site Characterization Methods for Discontinuous Permafrost Terrain, Environment and Natural Resources, Government of the Northwest Territories.

Waterline Resources Inc. (2013a). 2013 Shallow Environmental Investigation Slater River Project Near Norman Wells, Northwest Territories.

Waterline Resources Inc. (2013b). Slater River Project Groundwater Investigation Program 2013 Winter Mud-Rotary Drilling Summary Report.